Anal. Methods Environ. Chem. J. 8 (4) (2025) 160-174

AMECJ

Research Article, Issue 4
Analytical Methods in Environmental Chemistry Journal
Journal home page: www.amecj.com/ir

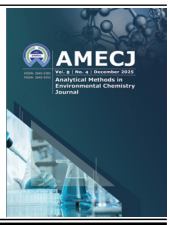

Rapid lead and cadmium adsorption from aqueous solutions using modified chitosan with citric acid before analysis by flame atomic absorption spectrometry

Khaled. W. Shuker[b], Hanadi A. Fadhil[a], Zainab H. Mohammed[b], Juman A. Naser[a,*], and Ahmed L. Majeed[c]

[a]*University of Baghdad, College of Education for Pure Science- Ibn Alhaitham, Department of Chemistry, Iraq- Baghdad*
[b]*Ministry of Education, Iraq- Baghdad*
[c]*Ministry of Industry and Minerals, Iraq- Baghdad*

ARTICLE INFO:

Received 5 Aug 2025
Revised form 16 Oct 2025
Accepted 12 Nov 2025
Available online 30 Dec 2025

Keywords:
Lead,
Cadmium,
Adsorption,
Chitosan,
Citric Acid,
Isotherm,
Flame atomic absorption spectrometry

ABSTRACT

In this research, a modified chitosan (NH_2-CS-COOH) with natural citric acid was used for the adsorption and removal of lead (Pb^{2+}) and cadmium (Cd^{2+}) ions in the liquid phase. Scanning electron microscopy (SEM), Fourier transform infrared spectroscopy (FTIR), and X-ray diffraction (XRD) were achieved using the sorbent. The concentrations of Cd(II) and Pb(II) ions were determined by flame atomic absorption spectrometry (F-AAS). Parameters in batch adsorption were studied, including adsorbent amount, contact time, concentration, and temperature. Optimized conditions were obtained for lead and cadmium using 10 mg and 20 mg of adsorbent (NH_2-Cs-COOH), respectively. Also, the contact times of 105 min for lead and 120 min for cadmium were obtained with an initial concentration of 10 mg L^{-1}. The data showed a better agreement with the Langmuir model, indicating maximum adsorption capacities (q_{max}) of 3.18 mg g^{-1} and (q_{max}) of 2.07 mg g^{-1} for lead and cadmium ions, respectively. Thermodynamic studies confirmed that the process is exothermic with negative ΔG° values. The results demonstrate that the adsorbent is highly effective for removing heavy metals from polluted water.

1. Introduction

Water pollution is a serious environmental and human challenge and affects the safety and sustainability of water sources [1]. The heavy metals [lead (Pb), cadmium (Cd), arsenic (As_V), and mercury (Hg)] with high toxicity and non-biodegradable properties can be accumulated in living tissues [2,3]. Heavy metals are found in mining and the chemical industry [4,5]. Even at low concentrations, it leads to serious health problems in humans (CNS disorders, kidney and liver damage, and cancer) [5-7]. Many technologies try to remove these elements from wastewater before it is released into the environment, which is essential for protecting the environment and human health. So, the various physical and chemical techniques were used to treat water contaminated with heavy metals (precipitation, ion exchange, osmosis, and filtration) [8-11]. However, some of these methods have disadvantages, such as high costs, expensive instrumentation and materials, and the generation of large amounts of sludge [12]. Therefore, the adsorption method is the most attractive technology, offering high efficiency, ease of use, low cost, and simple design [13]. This technology led to the development of effective and environmentally friendly adsorbents. Chitosan is a natural polymer

*Corresponding Author: Juman A. Naser
Email: juman.a.n@ihcoedu.uobaghdad.edu.iq
https://doi.org/10.24200/amecj.v8.i04.1111

that was derived from the deacetylation of chitin as an adsorbent. Chitosan contains active hydroxyl (-OH) and amine (-NH_2) groups and can bind heavy metal ions by its sites [14,15]. Chitosan is considered a good adsorbent because it is biodegradable, non-toxic, and less costly than other adsorbents. Chitosan can be chemically modified to enhance its properties, such as increasing surface area (SA)and improving physical and chemical properties [16,17]. Recently, many papers have shown the efficiency of chitosan in adsorbing or removing heavy metals such as cadmium, lead, and mercury. Jha and Iyengara demonstrated highly efficient adsorption of Cu(II) and Cd(II) ions in water and various matrices [18]. Rajesh et al. reported that the synthesis of chitosan gels using glutaraldehyde can increase lead adsorption capacity by more than 40% compared to native chitosan [19]. The hybrid materials were utilized by Krishna Kumar et al. They use chitosan/reduced graphene oxide (CS-rGO) with a high surface area for arsenic removal. CS-rGO had more adsorption sites and increased the removal efficiency to more than 95% [20]. However, there is still a need for new chemical modifiers or functionalization of adsorbents or for innovative synthesis of adsorbents to improve removal efficiency, the kinetic and thermodynamic properties. Despite the widespread use of modified chitosan, inexpensive natural sources, such as lemon juice (citric acid), have not received enough attention in the literature. Recently, various adsorbents, such as mesoporous silica nanoparticles, task-specific ionic liquids, nanographene oxide-modified phenyl methanethiol nanomagnetic composite, multi-walled carbon nanotubes, and Fe3O4-supported naphthalene-1-thiol-functionalized graphene oxide, have been used for the removal or adsorption of heavy metals in different matrices [21-32].

In this work, a simple, efficient, and environmentally friendly method was used to prepare chitosan modified with natural citric acid as an innovative adsorbent (NH_2-CS-COOH). It enhances the adsorbent's capacity for removing Cd and Pb ions. The conditions were optimized for the adsorption process (e.g., contact time, concentration, and adsorbent amount). The thermodynamics of the adsorption process, such as Langmuir and the Freundlich, were studied and evaluated.

2. Materials and Methods

2.1. Chemicals and Instrumental

Chitosan (purity ≥ 95%, average molecular weight 190 kDa) was used. Fresh lemon juice (Citrus aurantifolia) was used as the natural source of citric acid. Standard of lead nitrate [$Pb(NO_3)_2$] solution in HNO_3 2% with CAS Number: 10099-74-8 purchased from Sigma-Aldrich and suitable for atomic absorption spectrometry. Cadmium (Cd) metal dissolves readily in HNO_3 and HCl with a CAS number of 7440-43-9. A standard solution of Ca and Pb, based on high-purity (99%) reagents, was used to prepare calibration solutions of different concentrations. All solutions were prepared using double-purified distilled water. All chemicals used in this research were obtained from Sigma-Aldrich. HNO_3 (CAS Number: 7697-37-2), HCl (CAS Number: 7647-01-0), and H_2SO_4 (CAS Number: 7664-93-9) were purchased from Sigma, Germany. Ethanol or Ethyl alcohol with a purity of more than 99% (CAS Number: 64-17-5) and NaOH (CAS Number: 1310-73-2; EC Number: 215-185-5) were purchased from Sigma.

Flame atomic absorption spectrometry (F-AAS, GBC 902) provides good sensitivity and a low LOD for the analysis of Pb and Cd in water samples. A hollow-cathode lamp for Cd and Pb metals and an air–acetylene flame were used to atomize analytes. Calibration standards are prepared with different concentrations of Cd and Pb ions in solution, and absorbance is measured at 283.3 nm for Pb and 228.8 nm for Cd. Samples are introduced to a nebulizer–spray chamber to generate an aerosol for atomization. The GBC 902 was used with low LOD and high sensitivity for the analysis of environmental samples. The method enables the analysis of trace Pb and Cd in water samples. In this study, the Kuhner shaker (Germany) with stable speed control was used to homogenize samples before F-AAS analysis. A Thermo Scientific centrifuge (ST8/Megafuge Compact, USA) with digital control was used to separate phases and efficiently collect denser material at the bottom.

2.2. Preparation of adsorbent (modified chitosan)

2.2.1. Preparation of lemon juice extract

Fresh lemons were purchased, and the juice was manually prepared and filtered more than 3 times through a Wathman filter (0.5 µm). After filtration, the pulp and suspended solids were removed from the juice. Therefore, the obtained citric acid concentration was determined by the titration method (0.1 M NaOH and phenolphthalein). This citric acid was transferred into a glass and stored at -4 °C.

2.2.2. Chemical Modification

2.0 g of chitosan was added to 100 mL of lemon extract (pH < 3.0). The mixture was heated at 65°C under reflux for 90 min. After stirring the mixture, the chitosan chains were protonated with citric acid, and the mixture was cooled to 20 °C. Then, pH was adjusted to a basic range (pH> 10) with 1.0 M NaOH, which caused precipitation of the modified chitosan and created crosslinking between the COOH groups of citric acid and the NH2 groups of chitosan. The solid product was filtered and washed several times with an ethanol–water mixture (70:30%, v/v) to remove impurities. The product was dried for 1 day in an oven at 60 °C, sieved to obtain a 50–100 µm for the adsorption process (Schema 1).

2.3. Characterization

The NH_2-CS-COOH adsorbent was studied using scanning electron microscopy (SEM), Fourier transform infrared spectroscopy (FTIR), and X-ray diffraction (XRD) to analyze surface morphology, functional groups, and crystalline structure.

2.4. Adsorption Procedure

All adsorption process were studied using a batch technique in a vibrating incubator (HYSC SWB-25/Korean) set at 180 rpm. For Pb^{2+} adsorption, the standard conditions were: initial concentration 10 mg L^{-1}, adsorbent dosage 10 mg, temperature 25 °C, and contact time 105 minutes. For Cd^{2+} adsorption, the same initial concentration (10 mg L^{-1}) and temperature were used, but with a higher dosage (20 mg) and a contact time (120 minutes). Pb and Cd can be extracted from water samples based on NH_2-CS-COOH at pH 6.5 (Recovery > 70%). After shaking, the suspensions were filtered, and the remaining metal ion concentrations were measured to determine removal efficiency and adsorption capacity. The adsorption of Pb^{2+} and Cd^{2+} onto the NH_2-CS-COOH occurs through surface functional groups. The adsorbent of CS contains abundant –NH_2, –OH, and –COOH groups that become activated at pH 6.5. First, the metal ions bind to the adsorbent surface, where they interact with negatively charged (COO^-, OH^-) at pH 6.5. So, the electrostatic attraction created between Pb and Cd ions with functional groups of adsorbent, such as NH_2 and COOH groups (Schema 2). The adsorbent was separated from the solution by centrifugation at 180 rpm for 10 minutes. The residual metal was filtered twice and then measured using F-AAS at wavelengths of 283 nm for lead and 229 nm for cadmium. Also, the adsorption capacity was calculated q_e (mg g^{-1}) by Equation 1[33].

$$q_e = \frac{(C_o - C_e)V}{m} \quad \text{(Eq.1)}$$

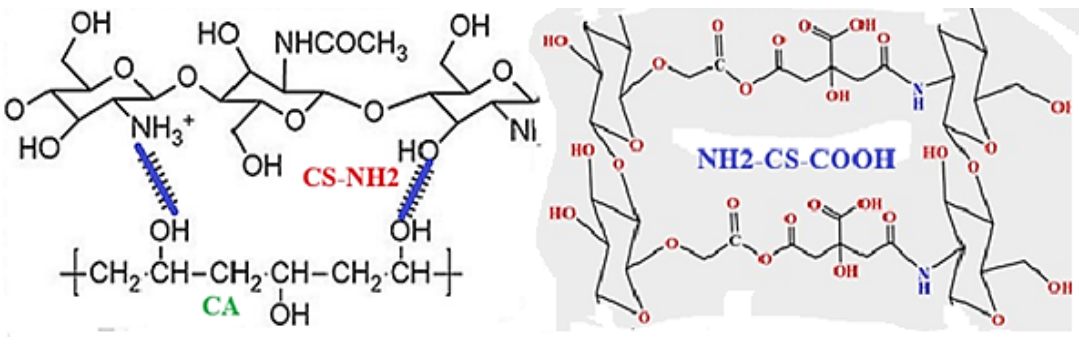

Schema 1. Modification of chitosan with citric acid

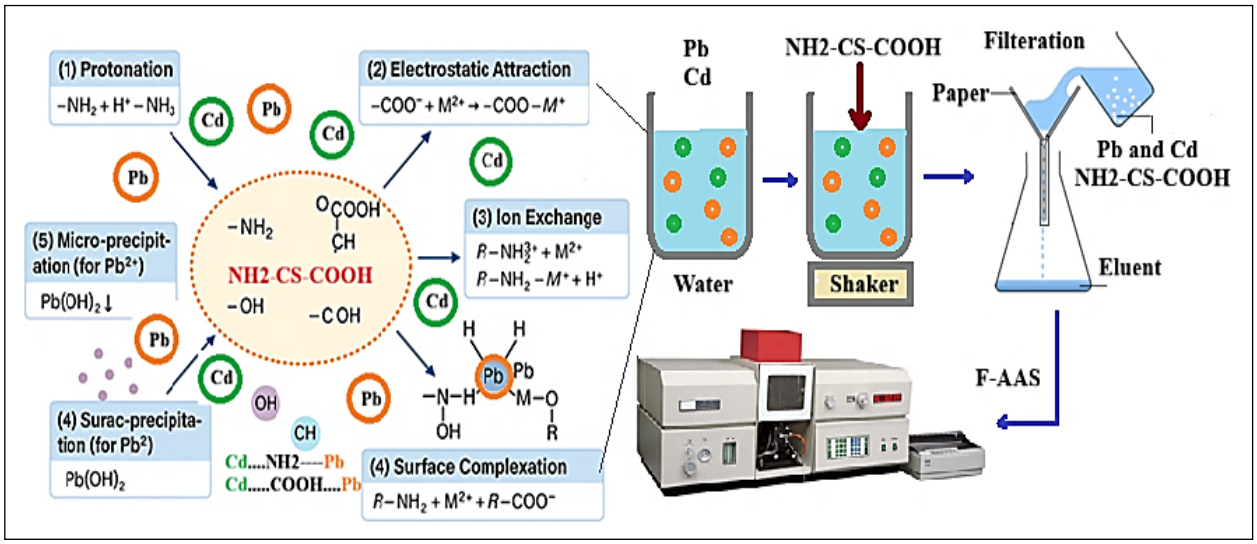

Schema 2. Procedure and mechanism for the extraction of Cd and Pb ions by NH_2-CS-COOH

where C_e is the ion concentration at equilibrium (mgL^{-1}), C_o is the initial ion concentration (mgL^{-1}), m is the mass of adsorbent (g), and *V* is the volume of salt solution (L).

3. Results and Discussion

To optimize adsorption conditions, the effect of each variable was studied individually, including adsorbent dosage within the range of 10 to 50 mg L^{-1}, contact time at different intervals (15, 30, 45, 60, 75, 90,105, and 120 minutes), initial concentration within 10 to 50 mg L^{-1}, pH levels from 2 to 11, and temperature at 298, 308, and 318 °C, while holding other factors constant.

3.1. Characterization of the Adsorbent

Various characterization techniques confirmed the successful preparation of chitosan modified with natural citric acid.

3.1.1.Scanning electron microscopy (SEM)

SEM images of NH_2-CS-COOH showed that the modified material had a rougher, more porous surface than pure chitosan (left, 1.0 micrometers) (Fig.1). This change is attributed to the successful modification process, which provides additional binding sites and facilitates the diffusion of metal ions (right, 500 nm).

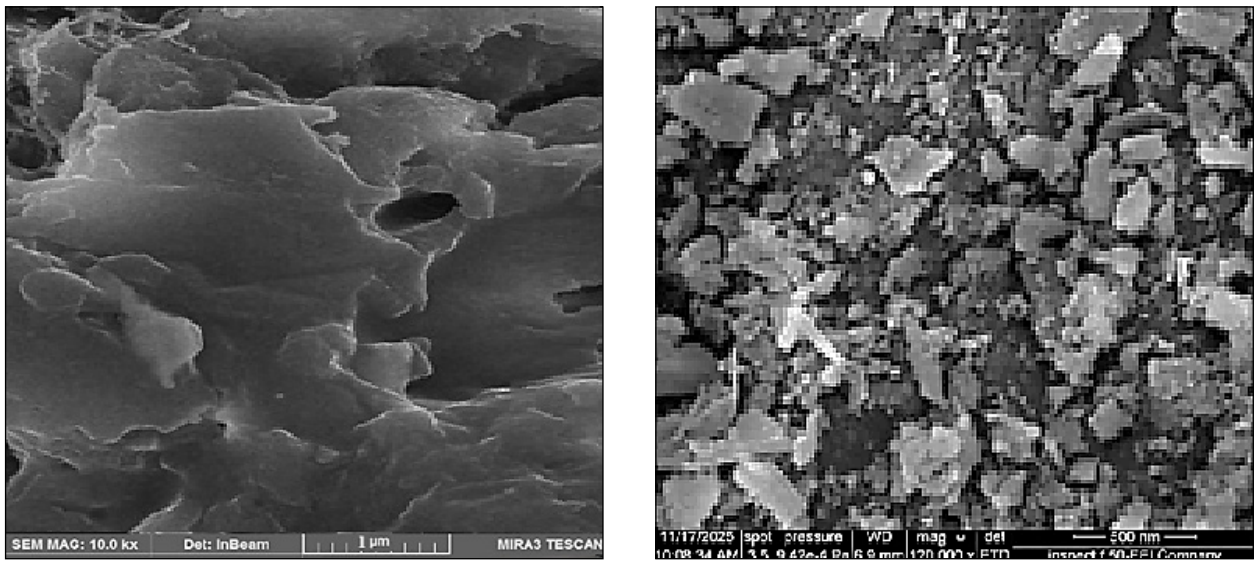

Fig. 1. SEM image of pure chitosan (left) and modified chitosan with natural citric acid (right)

3.1.2.X-ray diffraction (XRD)

XRD analysis of NH_2-CS-COOH showed a new peak at 2θ = 23° (Fig. 2), indicating a change in the crystal structure and the successful modification of chitosan by citric acid (Fig. 2). The XRD shows a broad peak instead of sharp crystalline peaks, indicating that chitosan becomes highly amorphous after modification. The weak peak near 2θ ≈ 10–20° is related to residual semicrystalline regions of chitosan (reduced by cross-linking with citric acid). Citric acid introduces esterification and H-bond rearrangements and decreases crystallinity. So, the reduction in peak intensity and the broad background confirm successful chemical modification and increase surface activity for metal adsorption.

3.1.3.Fourier transform infrared (FTIR)

Modification of chitosan with citric acid was confirmed using Fourier transform infrared spectroscopy (FTIR). The spectrum of the NH_2-CS-COOH changes compared to pure chitosan, specially a significant weakening of the peak at 1587 cm^{-1} (Fig.3). This peak is related to the N-H bending vibration (-NH_2) in chitosan, and its disappearance in NH_2-CS-COOH is strong evidence for the participation of these groups. Also, a new peak at 1726 cm^{-1} was observed in the spectrum of the NH_2-CS-COOH, related to the C=O stretching vibration (free carboxyl groups, -COOH). New changes were also observed in the amide region, with peaks at ~1620 cm^{-1} (amide I) and 1535 cm^{-1} (amide II),

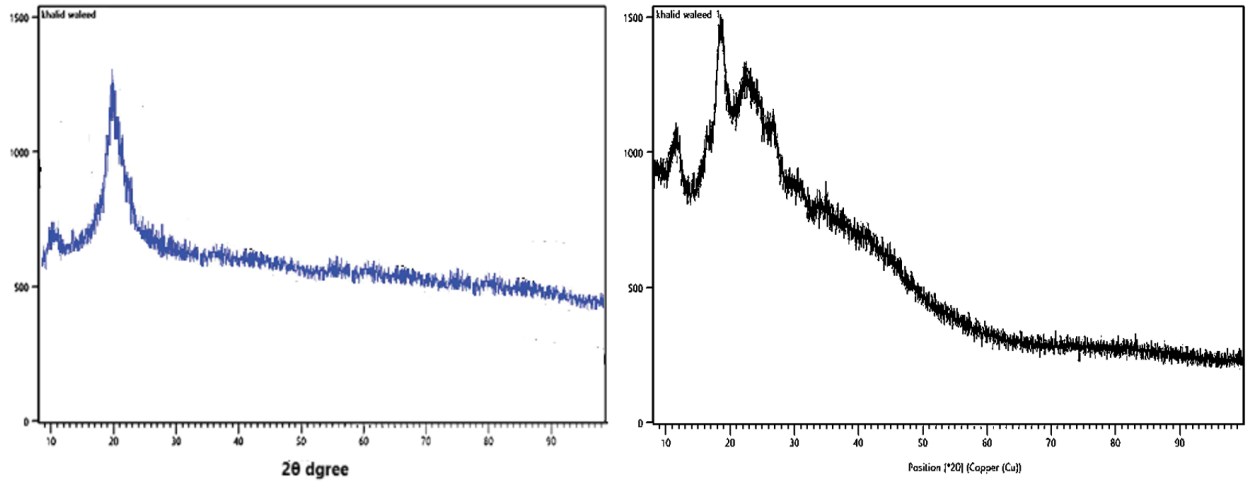

Fig. 2. XRD spectrum of chitosan (left) and modified chitosan with natural citric acid(right)

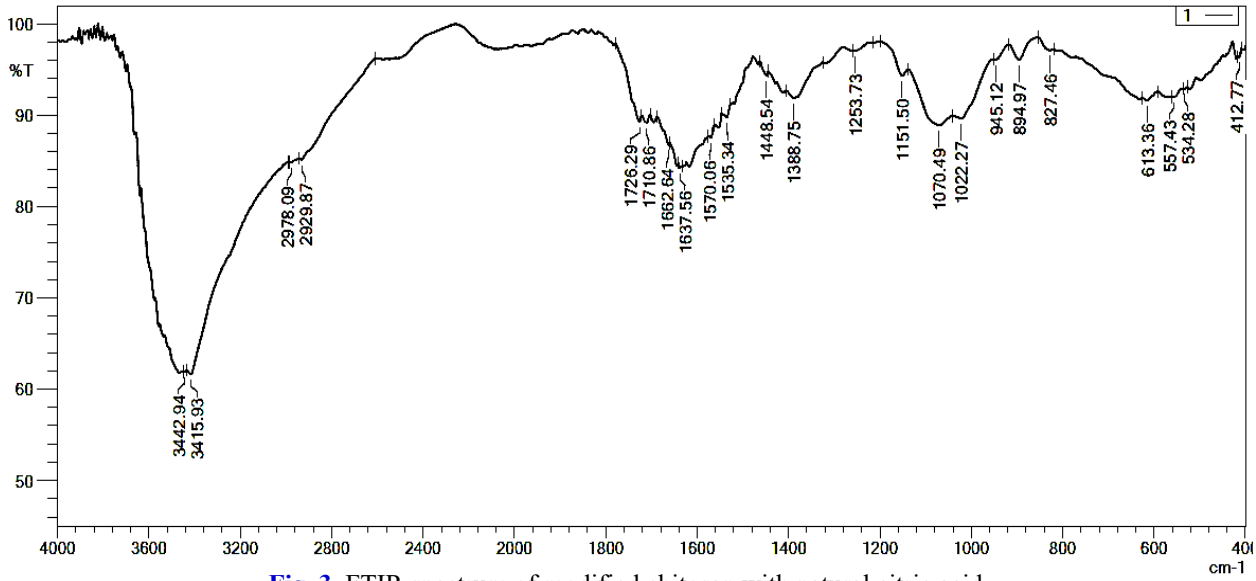

Fig. 3. FTIR spectrum of modified chitosan with natural citric acid.

corresponding to a combination of N-H bending and C-N stretching vibrations. The broad band in the 3350–3450 cm^{-1} region indicates enhanced H-bonding between the OH and COOH groups of the NH2-CS-COOH. In addition, the C-O-C glycosidic bond peak at ~1022 cm^{-1} confirms that the modification process preserved the structural of the chitosan's framework.

3.2. Factors affecting on adsorption

3.2.1.Effect of adsorbent dose

Effect of amount of adsorbent of NH2-CS-COOH on Cd and Pb adsorption and removal was shown in Figure 4. Due to results [34], the removal efficiency increased with adding dosage of NH2-CS-COOH from 0.005 to 0.02 g L^{-1} (5-20 mg adsorbent). Results showed that the optimal amount for Pb is 0.008 to 0.01 g L^{-1} (10 mg adsorbent). However, the adsorption capacity (mg g^{-1}) can be decreased with increasing dosage. Low absorption capacity related to incomplete usage of all adsorption sites or agglomeration of adsorbent molecules. Based on these results, an amount of 0.01 g L^{-1} (10 mg) was selected as the optimal amount for lead (Recovery 68-72%) and 0.02 g L^{-1} (20 mg) was chosen for cadmium (Recovery between 70-75).

3.2.2.Effect of contact time

The effect of contact time on the adsorption of Pb^{2+} and Cd^{2+} ions onto NH2-CS-COOH was investigated under the optimized conditions (Fig. 5). The adsorption capacity increased rapidly during the initial stage of the process. It is related to the large number of available active sites on the NH2-CS-COOH surface. Also, the adsorption rate gradually decreased on NH2-CS-COOH surface. The contact time at 105 minutes for Pb^{2+} and 120 minutes for Cd^{2+} reached equilibrium. After this time, the adsorption capacity has negligible changes [35]. The different times are related to differences in the ionic properties of the adsorbates. Cd^{2+} ions have a slightly longer time to reach surface saturation. The fast adsorption stage is mainly dependent on film diffusion, while the later stage is controlled by intraparticle diffusion as ions migrate deeper into the NH2-CS-COOH surface pores.

3.2.3.Effect of initial concentration

The effect of the initial metal concentration on chitosan adsorption was examined from 10mg L^{-1} to 50 mg L^{-1}. Figures 6a and 6b showed that the adsorption capacity (q_e) increased with increasing initial concentration for both Pb^{2+} and Cd^{2+}. This behavior is attributed to the greater driving force for mass transfer from the bulk solution to the adsorbent surface at higher concentrations. However, the percentage removal (%R) decreased gradually with increasing initial concentration. At lower concentrations (10 mgL^{-1}), a large number of

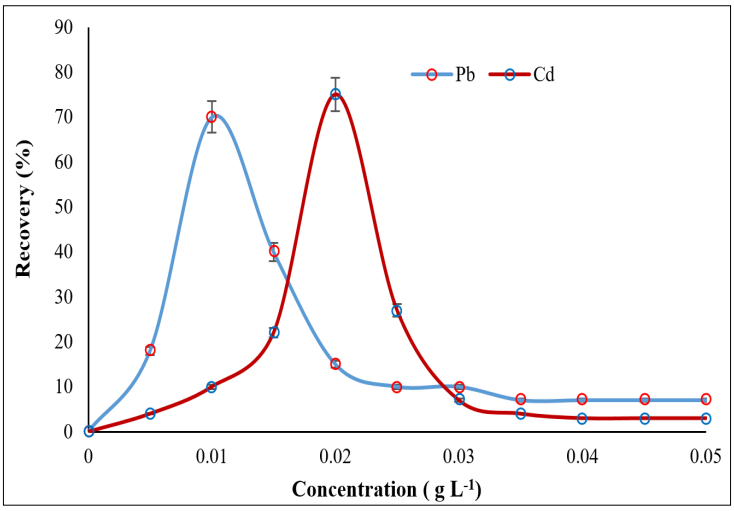

Fig. 4. Effect of adsorbent dose on the adsorption of lead and cadmium ions on the surface of modified chitosan with citric acid.

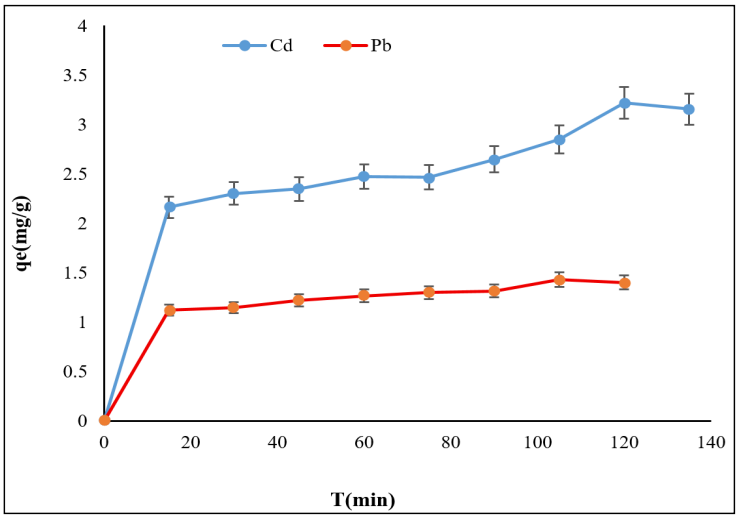

Fig. 5. Contact time effect of adsorption of lead and cadmium ions on the surface of modified chitosan with citric acid.

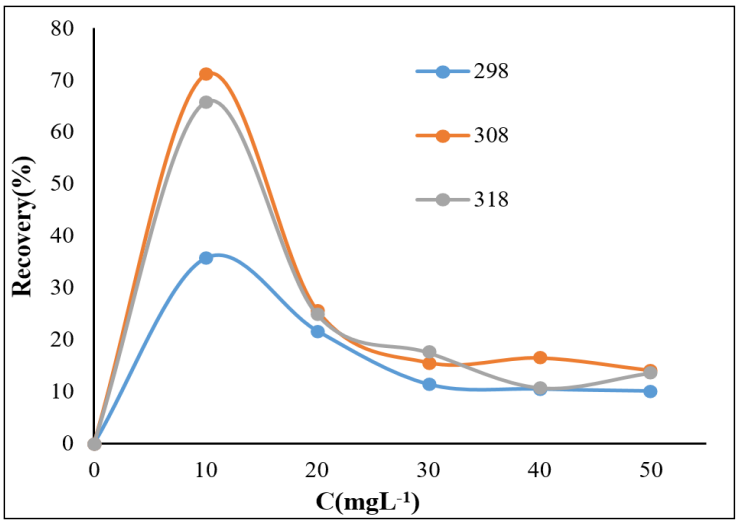

Fig. 6b. Initial concentration effect of the adsorption of lead ions on the surface of modified chitosan with citric acid.

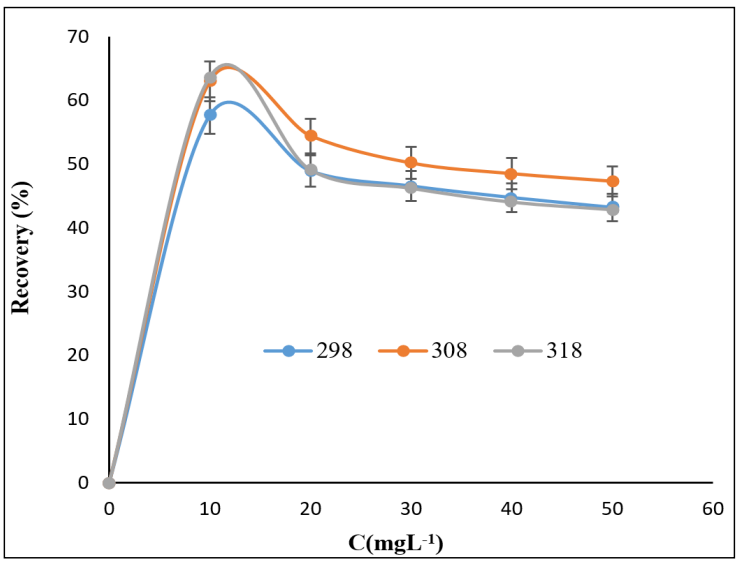

Fig.6a. Initial concentration effect of adsorption of cadmium ions on the surface of modified chitosan with citric acid.

active sites on the chitosan surface are available, resulting in high removal efficiencies (more than 70% for Pb^{2+} and Cd^{2+}). As the concentration increases, these active sites become progressively saturated, reducing removal efficiency (≈20–30% at 50 mg L^{-1}). The higher adsorption efficiency of Pb^{2+} compared to Cd^{2+} can be related to its greater polarizability and lower hydration energy [36]. These results confirm that the adsorbent surface becomes saturated more rapidly at higher Pb and Cd concentrations.

3.2.4.Effect of pH

Pb and Cd in the liquid phase can be extracted from water samples using NH_2-CS-COOH at optimized pH levels. The adsorption of Pb^{2+} and Cd^{2+} onto the surface of NH_2-CS-COOH occurs through physicochemical interactions involving functional groups at a suitable pH. The chitosan (CS) adsorbent contains abundant $–NH_2$, –OH, and –COOH groups that become activated at neutral pH. Therefore, the effects of pH on the extraction of Pb and Cd were studied at pH 2 and 11(Fig.7). The results indicated that Cd^{2+} and Pb^{2+} ions, which have positive charges, interact with negatively charged carboxylate groups ($–COO^-$) and deprotonated OH^- and NH_2^- groups at pH 6-7. Consequently, the extraction relies on electrostatic attraction, which facilitates the surface binding of Pb and Cd ions to functional groups such as NH_2 and COOH. The procedure achieves efficient recovery of Cd^{2+} and Pb^{2+} ions via ion-exchange extraction, primarily via the amino and carboxyl groups of chitosan at pH 6.5. In fact, the formation of inner-sphere surface adsorbent complexes with Pb^{2+} or Cd^{2+} modifies the binding strength of metal adsorption. Additionally, Pb and Cd precipitate at pH levels above 8.0, promoting the partial formation of $Pb(OH)_2$ and $Cd(OH)_2$.

3.3. Adsorption Isotherms

To further understand the interaction of lead and cadmium ions with the adsorbent surface, equilibrium data were analyzed using the Langmuir and the Freundlich models [37], as shown in Equations 2 and 3, respectively. Figures 8 and 9 show the Langmuir equation values (qmax, K_L, and plotting Ce/qe against Ce). Also, Figures 10 and 11 show the Freundlich parameters (kf, n, and slope of a plot of lnqe against lnCe).

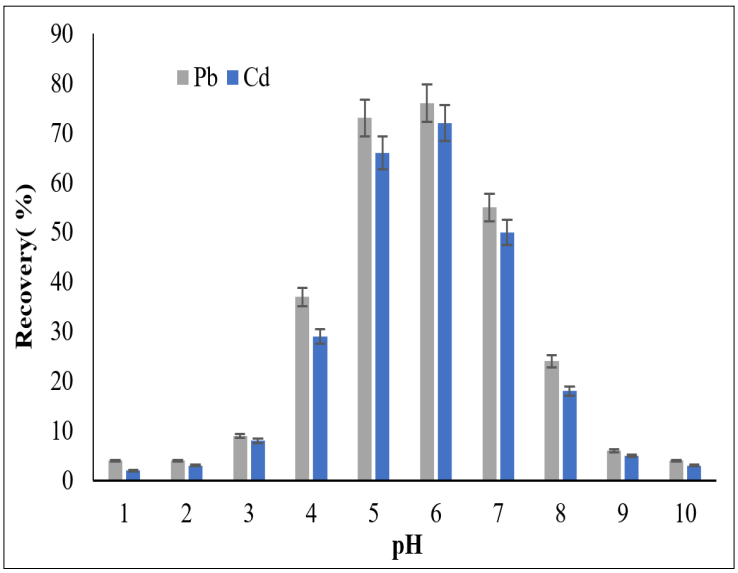

Fig.7. Effect of pH on the extraction of Pb and Cd by NH_2-CS-COO

$$(\frac{C_e}{q_e}) = \frac{1}{q_{max}k_L} + \frac{C_e}{q_{max}}$$

(Eq.2)

The q_e is the quantity of ions at equilibrium (mg g^{-1}). Ce is the concentration of ions (mg L^{-1}). qmax is the maximum adsorption capacity. K_L is the Langmuir experimental constant. The slope of the line represents $q_{max,}$ and K_L is the intercept.

$$lnq_e = lnk_f + \frac{1}{n}lnC_e$$

(Eq.3)

Where q_e is the amount of adsorbed ions at equilibrium (mg g^{-1}), C_e is the adsorbed concentration of ions at equilibrium (mgL^{-1}), both k_f and n are experimental constants of the Freundlich isotherm.

The Langmuir model showed better agreement with the experimental data than the Freundlich model, with coefficients of determination (R^2) of 0.99 and 0.81 for lead and cadmium, respectively. This indicates that the adsorption process occurs on a homogeneous surface in a monolayer with a limited number of active sites of similar energy [38], suggesting that all adsorption sites have approximately the same ion-binding capacity. The q_{max} for lead and cadmium were calculated using the Langmuir model and found to be 3.18 mg g^{-1} and 2.07 mg g^{-1}, respectively.

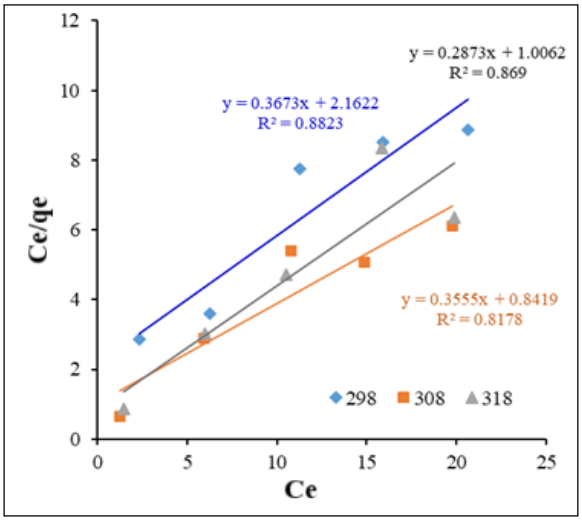

Fig. 8. Langmuir isotherms of Pb adsorption

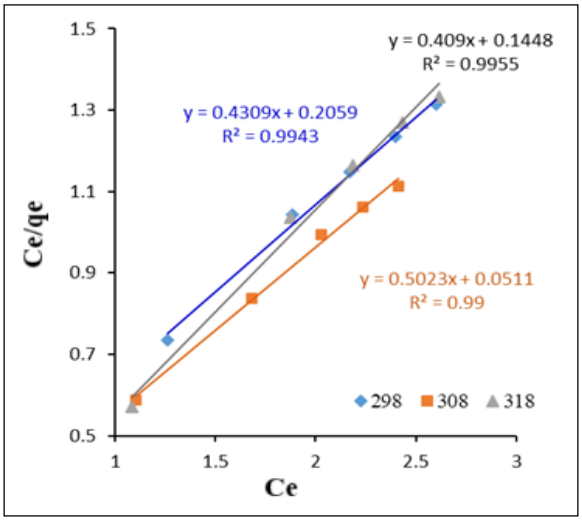

Fig. 9. Langmuir isotherms of Cd adsorption

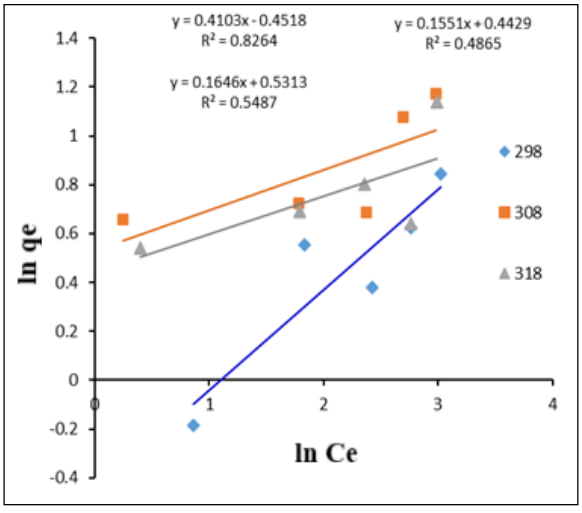

Fig.10. Freundlich isotherms of Pb adsorption

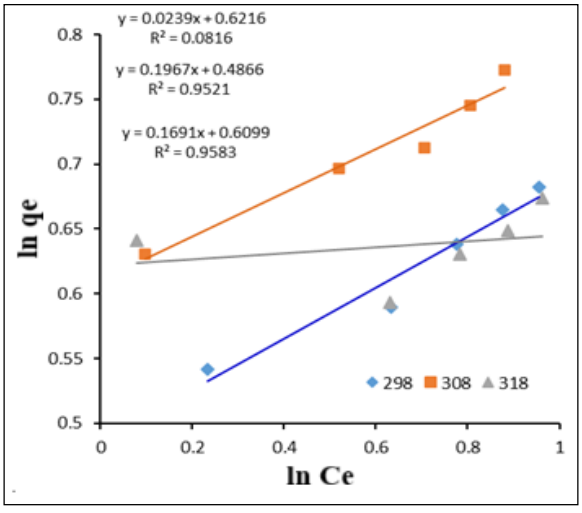

Fig. 11. Freundlich isotherms of Cd adsorption

These reported values are higher than the conventional pure chitosan adsorbents (≈ 1.6 mg g^{-1}) [39]. The higher adsorption capacity (AC) of lead compared to cadmium is related to differences in ionic radius and polarizability. The Langmuir separation coefficient (R_L) ranged between 0.81 and 0.99. R_L indicates that the adsorption process is thermally preferred ($0 < R_L < 1$). In fact, this means that the ions naturally move towards the material's surface without requiring high external energy. So, the adsorption mechanism is based on van der Waals forces and electrostatic attraction, rather than on covalent bonds [40]. The results showed that the NH_2-CS-COOH adsorbent is highly efficient at removing Pb and Cd ions from aqueous solutions. [41]. Due to high AC and the physical adsorption of NH_2-CS-COOH adsorbent, conformity with the Langmuir model is facilitated.

3.4. Thermodynamics of Adsorption

The effect of temperature on adsorption was investigated at 298, 308, and 318 K. The thermodynamic functions were continuously calculated using the following path of mathematical Equations 4 [42]. This equation uses the Kelvin temperature unit (T), the universal gas constant (R), the thermodynamic equilibrium constant (K), and the enthalpy change of adsorption (ΔH). The slope of the straight line in Figure 12, obtained by plotting lnK against 1/T (van't Hoff plot), was used to calculate the enthalpy shift. An estimate of the free Gibbs energy, it, was obtained using Equation 5 [43]. Due to Equation 6, an equilibrium Gibbs formula was used to estimate the value of entropy changes (ΔS°) [44].

The results, Tables 1 and 2 showed that the adsorption capacity of cadmium decreased with increasing temperature (2.32 → 1.99 mg g^{-1}), indicating that the process is exothermic. Lead, on the other hand, exhibited irregular behavior with a general tendency to decrease at the highest temperature, further confirming that the adsorption was not endothermic [45].

$$lnK = \frac{-\Delta H}{RT} + constant \quad \text{(Eq.4)}$$

$$\Delta G^0 = -RTlnK \quad \text{(Eq.5)}$$

$$\Delta G^0 = \Delta H^0 - T\Delta S^0 \quad \text{(Eq.6)}$$

The negative values of the Gibbs free energy (ΔG°) indicate that the adsorption process was thermally spontaneous at all studied temperatures for cadmium (−1.21 to −1.64 kJ mol^{-1}) and for lead at 308 and 318 K (−1.36 to −1.17 kJ mol^{-1}). The increasing negativity with increasing temperature indicates that adsorption becomes more spontaneous within this temperature range. The enthalpy of adsorption (ΔH°) was negative for both cadmium (−7.28 kJ mol^{-1}) and lead (−4.32 kJ mol^{-1}), indicating that the adsorption is exothermic [46], meaning that the high temperature inhibits the binding of ions to the active sites due to the weakening of the physical forces involved (such as van der Waals forces or electrostatic bonds). The ΔS° values are negative for Cd (−20.4 to −17.8 J $mol^{-1}K^{-1}$) and Pb (−18.3 to −10 J mol^{-1} K^{-1}) [47]. The small values of |ΔH°| (less than 40 kJ mol^{-1}) and low |ΔG°| confirm that the adsorption mechanism is physisorption. So, efficient adsorption occurred at low temperatures.

Based on the results of characterization, equilibrium, and thermodynamics, it can be suggested that the mechanism of adsorption of lead and cadmium ions on citric acid-modified chitosan involves: (electrostatic attraction between positively charged ions and negatively charged groups on the modified surface, chemical entanglement between lone pairs of electrons on nitrogen (-NH_2) and oxygen (-OH) atoms and metal ions, surface deposition or ion exchange under certain conditions, and physical reactions such as ion diffusion within the material's pores) [48].

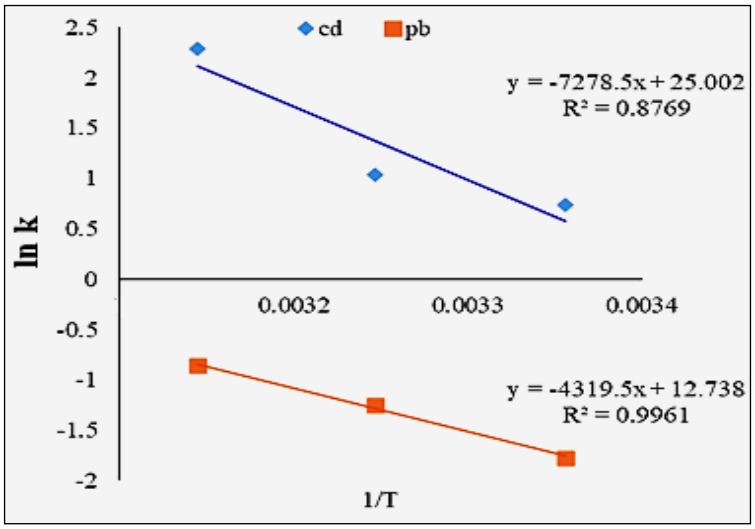

Fig.12. Represents the van't Hoff equation for the adsorption of lead and cadmium ions on the surface of modified chitosan with citric acid.

Table 1. values of thermodynamic functions for Pb adsorption on the surface of NH_2-CS-COOH

Temperature (K)	ΔH°(KJ mol^{-1})	ΔG°(KJ mol^{-1})	ΔS°(J mol^{-1}K^{-1})
298	-7.278	-1.2055	-20.3789
308		-1.5617	-18.5608
318		-1.6434	-17.7204

Table 2. values of thermodynamic functions for Cd adsorption on the surface of NH_2-CS-COOH

Temperature (K)	ΔH°(KJ mol^{-1})	ΔG°(KJ mol^{-1})	ΔS°(J mol^{-1}K^{-1})
298	-4.319	-1.1193	-18.2512
308		-1.3605	-9.60712
318		-1.1709	-9.90106

4. Conclusion

In this study, the potential of a hybrid material prepared from modified chitosan and natural citric acid as an effective adsorbent for removing heavy metal ions from aqueous solutions was successfully demonstrated. SEM, FTIR, and XRD confirmed the success of the modification process, resulting in a material with a rougher, more porous surface structure and new functional groups that support chemical reactions. The optimal conditions, such as dosage, contact time, and initial concentration, for the adsorption of Pb and Cd ions were at (10 mg and 20 mg), (105 min and 120 min), and 10 mg L^{-1}, respectively. The q_{max} for lead and cadmium ions were obtained at 3.18 mg g^{-1} and 2.07 mg g^{-1}, respectively. The concentrations of Pb and Cd in solutions were determined by flame atomic absorption spectrometry at pH 6.5. This recovery value (%) is significantly higher than that of unmodified chitosan. The adsorption data were better fit by the Langmuir model, indicating that adsorption occurs in a monolayer on a homogeneous surface. The thermodynamic study suggested

that the adsorption process is exothermic and spontaneous, as evidenced by negative ΔG° values (ranging from 1.1 to 1.6 kJ mol^{-1}) and by matrix/ disordered properties (ranging from 9.9 to 20.3 kJ $mol\ K^{-1}$). Based on the results, it can be concluded that the adsorption mechanism is a multi-stage process, dominated by the chemical cross-linking of metals with amine and hydroxyl groups, with electrostatic attraction and diffusion within the pores providing additional support. In summary, this study demonstrates that chitosan modified with natural citric acid is a promising, cost-effective, and environmentally friendly adsorbent for removing mineral pollutants from water.

5. References

[1] P.S. Bhavsar, S.S. Mishal, P.V. Devre, Evaluating the impact of urbanization and pollution on drinking water quality in Southern Gujarat: A study of physical, chemical, and microbial contaminants, Cleaner Water, 4 (2025) 100168. https://doi.org/10.1016/j.clwat.2025.100168

[2] R.S. Shammi, M.S. Islam, M.H. Kabir, Heavy Metal (loid) Pollution in the Laukhati River Water of Bangladesh: Environmental Implications for the Patuakhali Coastal Region, Cleaner Water, 4 (2025) 100170. https://doi.org/10.1016/j.clwat.2025.100170

[3] F. Meng, D. Liu, T. Bu, M. Zhang, J. Peng, J. Ma, Assessment of pollution and health risks from exposure to heavy metals in soil, wheat grains, drinking water, and atmospheric particulate matter, J. Environ. Manage., 376 (2025) 124448. https://doi.org/10.1016/j.jenvman.2025.124448

[4] V.G. Le, T.A. Luu, M.K. Nguyen, G.C. Nguyen, A. Q. Nguyen, N.T. Anh, D.D. Nguyen, Removal of heavy metals from battery industry effluents: recent progress and future perspectives for net-zero strategies and goals, J. Water Process Eng., 79 (2025) 108928. https://doi.org/10.1016/j.jwpe.2025.108928

[5] E. De Beni, W. Giurlani, L. Fabbri, R. Emanuele, S. Santini, C. Sarti, M. Innocenti, Graphene-based nanomaterials in the electroplating industry: A suitable choice for heavy metal removal from wastewater, Chemosphere, 292 (2022) 133448. https://doi.org/10.1016/j.chemosphere.2021.133448

[6] T.A. Alemayehu, A.M. Hiruy, M. Meles, B. Tefera, T.A. Terfie, Assessment of heavy metal exposure and cancer risk in Addis Ababa: Trends, risk factors and demographic variations in urinary cadmium, lead and chromium levels, Toxicol. Rep., 15 (2025) 102122. https://doi.org/10.1016/j.toxrep.2025.102122

[7] S. Kotnala, S. Tiwari, A. Nayak, B. Bhushan, S. Chandra, C.R. Medeiros, H.D.M. Coutinho, Impact of heavy metal toxicity on the human health and environment, Sci. Total Environ., 987 (2025) 179785. https://doi.org/10.1016/j.scitotenv.2025.179785

[8] Y.G. Ko, Hybrid method integrating adsorption and chemical precipitation of heavy metal ions on polymeric fiber surfaces for highly efficient water purification, Chemosphere, 363 (2024) 142909. https://doi.org/10.1016/j.chemosphere.2024.142909

[9] J. Sun, W. Cui, B. Liu, Y. Bai, Q. Zhang, B. Liu, J. He, Sulfonated graphene porous nanofiber membrane with ion exchange function for the removal of heavy metal ions from water, SSRN, 5332754. http://dx.doi.org/10.2139/ssrn.5332754

[10] H.Y. Yu, S. Gupta, Z. Zhou, Removal of metals and assimilable organic carbon by activated carbon and reverse osmosis point-of-use water filtration systems, Chemosphere, 365 (2024)143251. https://doi.org/10.1016/j.chemosphere.2024.143251

[11] Y. Alhammadi, A. Hai, H. Taher, F. Banat, F. AlMarzooqi, Enhancing heavy metals filtration: Synergistic effects of banana peel-derived activated carbon and layered double hydroxides in ultrafiltration membranes, Sep. Purif. Technol., 362 (2025) 131875. https://doi.org/10.1016/j.seppur.2025.131875

[12] L.S. Azmi, Membrane filtration technologies for sustainable industrial wastewater

treatment: A review of heavy metal removal, Desalination Water Treat. 323 (2025) 101321. https://doi.org/10.1016/j.dwt.2025.101321

[13] J.A. Naser, Z.W. Ahmed, E.H. Ali, Nanomaterials usage as adsorbents for the pollutants removal from wastewater: A review, Mater. Today Proc., 42 (2021) 2590–2595. https://doi.org/10.1016/j.matpr.2020.12.584

[14] K.X. Huang, L.Y. Zhou, J.Q. Chen, N. Peng, H.X. Chen, H.Z. Gu, T. Zou, Applications and perspectives of quaternized cellulose, chitin and chitosan: A review, Int. J. Biol. Macromol., 242 (2023) 124990. https://doi.org/10.1016/j.ijbiomac.2023.124990

[15] F. Hisham, M.H.M. Akmal, F. Ahmad, K. Ahmad, N. Samat, Biopolymer chitosan: Potential sources, extraction methods, and emerging applications, Ain Shams Eng. J., 15 (2024) 102424. https://doi.org/10.1016/j.asej.2023.102424

[16] S. Mirizadeh, A. Converti, A.A. Casazza, Chitosan-based adsorbents for antibiotic removal with insights from batch and dynamic studies: A review, Int. J. Biol. Macromol., 331 (2025) 148399. https://doi.org/10.1016/j.ijbiomac.2025.148399

[17] F. da Silva Bruckmann, J.O. Gonçalves, L.F.O. Silva, M.L.S. Oliveira, G.L. Dotto, C.R.B. Rhoden, Chitosan-based adsorbents for wastewater treatment: A comprehensive review, Int. J. Biol. Macromol., 309 (2025) 143173. https://doi.org/10.1016/j.ijbiomac.2025.143173

[18] I.N. Jha, L. Iyengar, A.P. Rao, Removal of cadmium using chitosan, J. Environ. Eng., 114 (1988) 962–974. https://doi.org/10.1061/(ASCE)0733-9372(1988)114:4(962)

[19] V. Rajesh, N. Rajesh, An indigenous Halomonas BVR1 strain immobilized in cross-linked chitosan for adsorption of lead and cadmium, *Int. J. Biol. Macromol.*, 79 (2015) 300-308. https://doi.org/10.1016/j.ijbiomac.2015.04.071

[20] A. S. Krishna Kumar, S.-J. Jiang, Chitosan-functionalized graphene oxide: A novel adsorbent an efficient adsorption of arsenic from aqueous solution, J. Environ. Chem. Eng., 4 (2016) 1698-1713. https://doi.org/10.1016/j.jece.2016.02.035

[21] F. Golbabaei, Z. Sadeghi, A. Vahid, A. Rashidi, On-line micro column preconcentration system based on amino bimodal mesoporous silica nanoparticles as a novel adsorbent for removal and speciation of chromium (III, VI) in environmental samples, J. Environ. Health Sci. Eng., 13 (2015) 1-12. https://doi.org/10.1186/s40201-015-0205-z

[22] A. Rashidi, A. Vahid, Arsenic speciation based on amine-functionalized bimodal mesoporous silica nanoparticles by ultrasound assisted-dispersive solid-liquid multiple phase microextraction, Microchem. J., 130 (2017) 137-146. https://doi.org/10.1016/j.microc.2016.08.013

[23] N. Esmaeili, J. Rakhtshah, Ultrasound assisted-dispersive-modification solid-phase extraction using task-specific ionic liquid immobilized on multiwall carbon nanotubes for speciation and determination mercury in water samples, Microchem. J., 154 (2020) 104632. https://doi.org/10.1016/j.microc.2020.104632

[24] M. K. Abbasabadi, F. Hosseini, Nanographene oxide modified phenyl methanethiol nanomagnetic composite for rapid separation of aluminum in wastewaters, foods, and vegetable samples by microwave dispersive, Food Chem., 347 (2021) 129042. https://doi.org/10.1016/j.foodchem.2021.129042

[25] M. Arjomandi, A review: analytical methods for heavy metals determination in environment and human samples, Anal. Methods Environ. Chem. J., 2 (2019) 97-126. https://doi.org/10.24200/amecj.v2.i03.73

[26] J. Rakhtshah, M. Dehghani Mobarake, Simultaneously speciation and determination of manganese (II) and (VII) ions in water, food, and vegetable samples based on immobilization of N-acetylcysteine on multi-walled carbon nanotubes, Food Chem., 389 (2022) 133124. https://doi.org/10.1016/j.foodchem.2022.133124

[27] S. Davari Ahranjani, A lead analysis based on

amine functionalized bimodal mesoporous silica nanoparticles in human biological samples by ultrasound assisted-ionic liquid trap-micro solid phase extraction, J. Pharm. Biomed. Anal., 157 (2018) 1-9.
https://doi.org/10.1016/j.jpba.2018.05.004

[28] K. Merchant, M. D. Mobarake, Ultrasound-assisted solid-liquid trap phase extraction based on functionalized multi-wall carbon Nanotubes for preconcentration and separation of nickel in petrochemical wastewater, J. Anal. Chem., 74 (2019) 865-876.
https://doi.org/10.1134/S1061934819090090

[29] A. F. Zarandi, An immobilization of 2-(Aminomethyl) thiazole on MWCNTs used for rapid extraction of manganese ions in hepatic patients, J. Pharm. Biomed. Anal., 240 (2024) 115941.
https://doi.org/10.1016/j.jpba.2023.115941

[30] N. Esmaeili, J. Rakhtshah, E. Kolvari, A. Rashidi, Rapid speciation of lead in human blood and urine samples based on MWCNTs@DMP by dispersive ionic liquid-suspension-micro-solid phase extraction, Biol. Trace Elem. Res., 199 (2021) 2496–2507.
https://doi.org/10.1007/s12011-020-02382-7

[31] M. K. Abbasabadi, Speciation of cadmium in human blood samples based on Fe_3O_4-supported naphthalene-1-thiol- functionalized graphene oxide nanocomposite by ultrasound-assisted dispersive magnetic micro solid phase extraction, J. Pharm. Biomed. Anal., 189 (2020) 113455.
https://doi.org/10.1016/j.jpba.2020.113455

[32] S. Davari, F. Hosseini, Dispersive solid phase microextraction based on amine-functionalized bimodal mesoporous silica nanoparticles for separation and determination of calcium ions in chronic kidney disease, Anal. Methods Environ. Chem. J., 1 (2018) 57-66.
https://doi.org/10.24200/amecj.v1.i01.37

[33] J.A. Naser, T.A. Himdan, A.J. Ibraheim, Adsorption kinetic of malachite green dye from aqueous solutions by electrospun nanofiber Mat. Orient. J. Chem, 33 (2017) 3121-3129.
http://dx.doi.org/10.13005/ojc/330654

[34] S.E. Hussain, J.A. Naser, Preparation and characterization of nickel oxide nanoparticles and its adsorption optimization for parachlorophenol, J. Med. Pharm. Chem. Res., 4 (2022) 1209–1217.
http://doi.org/10.22034/ecc.2022.348728.1492

[35] M.S. Çelik, O. Çaylak, N. Kütük, Removal of lead ions from aqueous solution using chitosan/starch composite material: Experimental and density functional theory findings, Biomass Conv. Bioref., 15, (2025) 1041–1056.
https://doi.org/10.1007/s13399-024-05287-w

[36] E. Hidayat, T. Yoshino, S. Yonemura, A Carbonized Zeolite/Chitosan Composite as an Adsorbent for Copper (II) and Chromium (VI) Removal from Water, Materials, 16 (2023) 2532;
https://doi.org/10.3390/ma16062532

[37] M.A. Al-Ghouti, D.A. Da'ana, Guidelines for the use and interpretation of adsorption isotherm models: A review, J. Hazard. Mater., 393 (2020) 122383.
https://doi.org/10.1016/j.jhazmat.2020.122383

[38] N. Ebelegi, N. Ayawei, D. Wankasi, Interpretation of adsorption thermodynamics and kinetics, Open J. Phys. Chem., 10 (2020) 166-182.
https://doi.org/10.4236/ojpc.2020.103010

[39] M. Saeid Rostami, M. M. Khodaei, Recent advances in chitosan-based nanocomposites for adsorption and removal of heavy metal ions, Int. J. Biol. Macromol., 270 (2024) 132386.
https://doi.org/10.1016/j.ijbiomac.2024.132386

[40] M. Benjelloun, Y. Miyah, G.A. Evrendilek, F. Zerrouq, S. Lairini, Recent advances in adsorption kinetic models: Their application to dye types. Arab. J. Chem., 14 (2021) 103031.
https://doi.org/10.1016/j.arabjc.2021.103031

[41] G. Crini, E. Lichtfouse, L.D. Wilson,

Conventional and non-conventional adsorbents for wastewater treatment, Environ. Chem. Lett., 17 (2019). 195-213. https://doi.org/10.1007/s10311-018-0786-8

[42] B. Wang, J. Lan, C. Bo, B. Gong, J. Ou, Adsorption of heavy metal onto biomass-derived activated carbon: A review, RSC Adv. 13 (2023) 4275–4302. https://doi.org/10.1039/D2RA07911A.

[43] K.H.H. Aziz, R. Kareem, Recent advances in water remediation from toxic heavy metals using biochar as a green and efficient adsorbent: A review, Case Stud. Chem. Environ. Eng., 8 (2023) 100495. https://doi.org/10.1016/j.cscee.2023.100495

[44] S.A. Razzak, M.O. Faruque, Z. Alsheikh, L. Alsheikhmohamad, D. Alkuroud, A comprehensive review on conventional and biological-driven heavy metals removal from industrial wastewater, Environ. Adv., 7 (2022) 100168. https://doi.org/10.1016/j.envadv.2022.100168

[45] B. Moghtaderi-Esfahani, K. Ghanemi, Thermodynamic, isothermal, and kinetic analysis of mercury (II) adsorption on marine sediments, Desalin. Water Treat., 321 (2025) 100921. https://doi.org/10.1016/j.dwt.2024.100921

[46] Z. Raji, A. Karim, A. Karam, S. Khalloufi, Adsorption of heavy metals: Mechanisms, kinetics, and applications of various adsorbents in wastewater remediation-A review, Waste, 1 (2023) 775–805. https://doi.org/10.3390/waste1030046

[47] L. Largitte, R. Pasquier, A review of the kinetics adsorption models and their application to the adsorption of lead by an activated carbon, Chem. Eng. Res. Des., 109 (2016) 495–504. https://doi.org/10.1016/j.cherd.2016.02.006

[48] S. Suguna Madala, S. Kumar Nadavala, Equilibrium, kinetics and thermodynamics of Cadmium (II) biosorption on to composite chitosan biosorbent, Arab. J. Chem., 10 (2017) S1883- S1893. https://doi.org/10.1016/j.arabjc.2013.07.017